Monthly Notices
of the
ROYAL ASTRONOMICAL SOCIETY

MNRAS **468,** 3682–3688 (2017)
Advance Access publication 2017 March 23

doi:10.1093/mnras/stx708

Discovery of a $z = 0.65$ post-starburst BAL quasar in the DES supernova fields

Dale Mudd,[1⋆] Paul Martini,[1,2] Suk Sien Tie,[1,2] Chris Lidman,[3] Richard McMahon,[4,5] Manda Banerji,[4,5] Tamara Davis,[6] Bradley Peterson,[1,2] Rob Sharp,[7,8] Nicholas Seymour,[9] Michael Childress,[10,11] Geraint Lewis,[12] Brad Tucker,[7,13] Fang Yuan,[7,11] Tim Abbot,[14] Filipe Abdalla,[15,16] Sahar Allam,[17] Aurélien Benoit-Lévy,[15,18,19] Emmanuel Bertin,[18,19] David Brooks,[15] A. Camero Rosell,[20,21] Matias Carrasco Kind,[22,23] Jorge Carretero,[24,25] Luiz N. da Costa,[20,21] Shantanu Desai,[26,27] Thomas Diehl,[17] Tim Eifler,[28,29] David Finley,[17] Brenna Flaugher,[17] Karl Glazebrook,[30] Daniel Gruen,[31,32] Robert Gruendl,[22,23] Gaston Gutierrez,[17] Samuel Hinton,[6] Klaus Honscheid,[2,33] David James,[14] Kyler Kuehn,[3] Nikolav Kuropatkin,[17] Edward Macaulay,[6] Marcio A. G. Maia,[20,21] Ramon Miquel,[25,34] Ricardo Ogando,[20,21] Andres Plazas,[29] Kevin Riel,[32] Eusebio Sanchez,[35] Basillio Santiago,[20,36] Michael Schubnell,[37] Ignacio Sevilla-Noarbe,[35] Robert C. Smith,[14] Marcelle Soares-Santos,[17] Flavia Sobreira,[20,38] Eric Suchyta,[39] Molly Swanson,[23] Gregory Tarle,[37] Daniel Thomas,[40] Syed Uddin,[30] Alistair Walker,[14] Bonnie Zhang[41] and The DES Collaboration

Affiliations are listed at the end of the paper

Accepted 2017 March 21. Received 2017 March 14; in original form 2016 June 6

ABSTRACT

We present the discovery of a $z = 0.65$ low-ionization broad absorption line (LoBAL) quasar in a post-starburst galaxy in data from the Dark Energy Survey (DES) and spectroscopy from the Australian Dark Energy Survey (OzDES). LoBAL quasars are a minority of all BALs, and rarer still is that this object also exhibits broad Fe II (an FeLoBAL) and Balmer absorption. This is the first BAL quasar that has signatures of recently truncated star formation, which we estimate ended about 40 Myr ago. The characteristic signatures of an FeLoBAL require high column densities, which could be explained by the emergence of a young quasar from an early, dust-enshrouded phase, or by clouds compressed by a blast wave. The age of the starburst component is comparable to estimates of the lifetime of quasars, so if we assume the quasar activity is related to the truncation of the star formation, this object is better explained by the blast wave scenario.

Key words: galaxies: active – quasars: absorption lines – galaxies: starburst.

1 INTRODUCTION

Correlations of the mass of the central supermassive black hole (SMBH) with host galaxy properties such as velocity dispersion (Gebhardt et al. 2000; Ferrarese & Merritt 2000) suggest that an SMBH's growth is linked to the evolution of the host galaxy through some feedback process (e.g. Heckman & Best 2014). The most pronounced phase of SMBH growth is the quasar phase, where most of the spectral energy distribution can be explained by a thin accretion disc of material around the SMBH (Shakura & Sunyaev 1973; Koratkar & Blaes 1999), a hot corona and a broad line region on larger scales (e.g. Peterson 1997). One method of triggering quasar activity is a merger that involves at least one gas-rich galaxy

⋆ E-mail: mudd@astronomy.ohio-state.edu

(Sanders et al. 1988; Silk & Rees 1998; Komossa et al. 2003; Di Matteo, Springel & Hernquist 2005; Piconcelli et al. 2010). During gas-rich mergers, gas funnels towards the central regions of the galaxies and some fraction accretes on to the central SMBH. This substantial influx of gas and dust may often obscure the early phases of quasar activity.

Gas-rich mergers also produce a large increase in star formation, up to 100–1000 times the galaxy's quiescent rate. These rates can quickly exhaust the gas supply, and eventually the star formation rate must return to a lower value. It is unclear if this is primarily caused by the expulsion of star-forming gas due to the quasar, feedback from the star formation process or consumption of the gas by star formation and the SMBH. If the increased star formation rate decreases quickly compared to the total star formation history, the galaxy goes through a post-starburst phase, which is characterized by the strong absorption lines prevalent in A-type stars combined with a K-type spectrum from an older population (Dressler & Gunn 1983; Zabludoff et al. 1996). The absence of stellar features due to shorter lived O- and B-type stars would indicate star formation ceased tens to hundreds of Myr ago. Some post-starburst galaxies also exhibit blueshifted absorption from winds (Tremonti, Moustakas & Diamond-Stanic 2007; Coil et al. 2011), and at least some wind-driven outflows from starbursts appear to be delayed by 10 Myr or more after the star formation burst (Sharp & Bland-Hawthorn 2010; Ho et al. 2016).

A significant fraction of all post-starburst galaxies host quasars (Brotherton et al. 1999, 2002; Cales et al. 2013) or some form of lower luminosity active galactic nuclei (AGN). Goto (2006) found that 0.2 per cent of all galaxies are in a post-starburst state, compared to 4.2 per cent of quasars having these post-starburst features. Quasars hosted by post-starburst galaxies typically had intense star formation that ended $10^{8–9}$ yr ago. Cales et al. (2013) found that older post-starburst quasars in elliptical galaxies tend to have signs of a recent merger, which suggests that a major merger event fuelled both the previous star formation and current quasar activity. Tremonti et al. (2007) and others argue that the presence of blueshifted absorption of a few hundred to a few thousand km s^{-1} in some post-starburst quasars is evidence that these objects had a large, galaxy-scale wind $\sim 10^8$ yr ago, although the energy in these winds may not be enough to have quenched star formation (Coil et al. 2011). Similar winds are seen in ongoing starbursts, but these tend to be a factor of a few weaker than in post-starbursts of comparable luminosity (Tremonti et al. 2007).

When the winds from a quasar are especially prominent, they are classified as broad absorption line (BAL) quasars. BALs are characterized by prominent, blueshifted absorption lines of 2000 km s^{-1} or more (Weymann et al. 1991). BALs are present in 20–40 per cent of all quasars, depending on the selection method (Trump et al. 2006; Dai, Shankar & Sivakoff 2008; Urrutia et al. 2009). The majority of BALs only exhibit absorption in high ionization states, such as C IV, and are referred to as HiBALs. BALs with absorption in lower ionization lines, such as Mg II, are referred to as LoBALs. A small subset of LoBALs also have Fe II and/or Fe III absorption and are known as FeLoBALs (Hazard et al. 1987). Rarest of all are the handful of objects with absorption in the Balmer lines (Hall 2007; Zhang et al. 2015). Using SDSS data, Trump et al. (2006) find that HiBALs, LoBALs and FeLoBALs constitute 26 per cent, 1.3 per cent and 0.3 per cent, respectively, of their sample of over 16 000 quasars. In contrast, Dai et al. (2008) and Urrutia et al. (2009) find BALs are much more common. When selected with both SDSS and 2MASS to alleviate the bias from reddening, they report 37 per cent, 32 per cent and 32 per cent of quasars are HiBALs, LoBALs and FeLoBALs, respectively. This selection method identifies all LoBALs as FeLoBALs.

FeLoBALs are the most heavily reddened BAL subtype, and the iron features necessitate high column densities (e.g. Korista et al. 2008). They can have broad iron emission and absorption from Fe III in addition to Fe II, and, in very rare cases, only Fe III (Hall et al. 2002). The absorption troughs are also observed to vary between objects from several distinct, narrow troughs, to blanketing most of the emission from the quasar shortward of the Mg II doublet. Both LoBALs and FeLoBALs also tend to be X-ray faint, further implying that there is a large column density that prevents a direct view of the central source (e.g. Mathur, Elvis & Singh 1995; Green et al. 2001).

There remains much debate about the exact nature of FeLoBALs. With their considerable reddening and high inferred column densities, some argue that they are transitional quasars, moving from a dust-enshrouded star formation phase to an unobscured quasar phase (Voit et al. 1993; Egami et al. 1996; Farrah et al. 2007, 2010). The highly absorbed FeLoBALs are also more likely to be radio sources, and may be transition objects between radio loud and radio quiet quasars (Becker et al. 1997). Alternatively, Faucher-Giguère, Quataert & Murray (2012) propose that the absorption is from high density clouds along the line of sight that have been disrupted by a blast wave from the SMBH, rather than a wind pushing out a dusty cocoon. This would create the absorbers *in situ*, allowing them to be either close to the central AGN or farther out in the galaxy but along our line of sight. The young, dust-enshrouded scenario is less flexible, as the absorbers should be within the central few parsecs.

We have discovered an FeLoBAL quasar with Balmer absorption and a post-starburst spectrum that was selected using data obtained by the Dark Energy Survey (DES; Flaugher 2005; Flaugher et al. 2015) and the OzDES[1] collaboration (Yuan et al. 2015). The quasar was found in one of the 10 'supernova fields' (3 deg^2 each, Kessler et al. 2015) that are monitored to discover Type Ia supernovae. OzDES obtains approximately monthly spectra of the 10 supernova fields with the AAOmega spectrograph (Smith et al. 2004; Sharp et al. 2006) on the 4m Anglo-Australian Telescope (AAT). Two of its main science goals are measuring redshifts for thousands of host galaxies of Type Ia supernovae discovered with DES photometry and repeatedly observing hundreds of quasars as part of a large-scale reverberation mapping project (King et al. 2015). OzDES also obtains spectra of various other classes of objects, including luminous red galaxies, BAL quasars and white dwarfs.

Several of the targets for the DES/OzDES reverberation mapping project are BAL quasars that were selected to monitor their long-term absorption and emission line variability. Upon stacking several spectra, we discovered that one of these objects, DES QSO J033049.33−283249.7 (hereafter DES QSO J0330−28), resides in a post-starburst galaxy. This appears to be the first known BAL quasar in a post-starburst galaxy. We also note that this is a FeLoBAL with Balmer absorption, making it rare even among BALs, and that it was first chosen as a target candidate from a combination of optical and infrared colour cuts described in Banerji et al. (2015) and reproduced below as equation (1):

$$\begin{aligned}(g-i)_{\rm AB} &< 1.1529 \times (i_{\rm AB} - K_{\rm Vega}) - 1.401\\ (W1-W2) &> 0.7\\ -0.003 < i_{\rm spreadmodel} &< 0.0028\\ i &< 21.5. \end{aligned} \quad (1)$$

[1] Australian Dark Energy Survey; alternatively, Optical redshifts for DES.

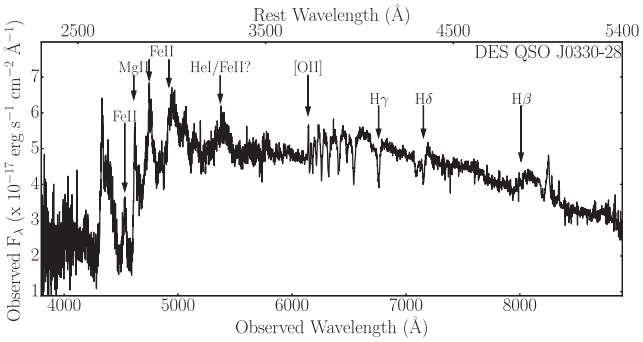

Figure 1. Stacked spectrum of DES QSO J0330−28 at $z = 0.65$. The LoBAL features are prominent at wavelengths shorter than the Mg II line at rest-frame 2798 Å. The absorption features around rest-frame 3900 Å are from host galaxy stars.

In Section 2, we describe the DES and OzDES observations and accumulate other values from the literature on this unique object. In Section 3, we characterize both the outflow and model the properties of the host galaxy stellar population using the stacked OzDES spectra. We summarize and present our conclusion in Section 4.

2 OBSERVATIONS

All of the spectra of DES QSO J0330−28 were obtained with the AAT 4m at Siding Spring Observatory as part of the OzDES project. The double beam fibre-fed spectrograph uses the 580V grating and 385R gratings leading to dispersions of 1 and 1.6 Å pixel^{-1} in the blue and red arms, respectively, with the dichroic split at 5700 Å. The resolution of the spectrograph is $R \sim 1400$, and the wavelength range spans 3700–8800 Å.

We present the stacked spectrum in Fig. 1 in both the observed and rest frame. This is a combination of four spectra taken over the course of 2 yr (2013–2015) and the combined exposure time is 160 min. We derived the host galaxy redshift of $z = 0.65$ based on the higher order Balmer lines around rest-wavelength 4000 Å. There is also a prominent Balmer break shortward of the absorption. These are the signs of a post-starburst galaxy with recently quenched star formation. At shorter wavelengths, there is a sharp drop in flux at the rest wavelength of the Mg II 2798 Å emission line. This corresponds to blueshifted absorption out to 5000 km s^{-1} from the systemic redshift. Other absorption troughs in the rest-frame UV correspond to metastable states of Fe II, particularly at 2750, 2880 and 2985 Å. There may be Mg I 2853 Å, but this falls in an Fe II absorption trough. The most common Fe III features are blueward of our spectral coverage.

We provide photometry for this object in Table 1. This incorporates *grizY* from DES, *JHK* from the Visual and Infrared Survey Telescope for Astronomy (VISTA) Hemisphere Survey (VHS; McMahon et al. 2013), and *W1*, *W2*, *W3*, *W4* from *WISE* (Wright et al. 2010). The DES and *WISE* magnitudes are calculated using PSF fits, whereas the VHS data use a 2 arcsec aperture. All magnitudes have been transformed to the AB system. Both the very red colours (e.g. $r - K = 0.86$ AB) and spectral shape indicate very substantial reddening, which is quite common with FeLoBALs (Hall et al. 1997, 2002; Dunn et al. 2015). The DES *g*, *r*, *i* and VISTA *K* images are shown in Fig. 2. These images show several small objects in the immediate vicinity of the quasar that suggest an interacting or merging system, and three of the objects have photometric redshifts consistent with DES QSO J0330−28. This quasar was also detected as a radio source in the Australia

Table 1. DES QSO J0330−28 photometry.

Band name	Cent. wave	Magnitude (error)
g	5720 Å	20.11 (0.02)
r	6590 Å	19.31 (0.02)
i	7890 Å	19.02 (0.02)
z	9760 Å	18.94 (0.02)
Y	1 μm	19.00 (0.02)
J	1.25 μm	18.89 (0.04)
H	1.65 μm	18.77 (0.05)
K	2.15 μm	18.45 (0.05)
W1	3.4 μm	17.64 (0.03)
W2	4.6 μm	17.01 (0.03)
W3	12 μm	15.92 (0.06)
W4	22 μm	15.01 (0.22)
ATLAS	1.474 GHz	256[a](20)

Notes. Photometry for DES QSO J0330−28 taken from DES for *grizY*, VHS for *JHK*(McMahon et al. 2013) and *WISE* for *W*1 − *W*4 (Wright et al. 2010). The DES data are PSF magnitudes obtained from the co-add of the first year of observations. All magnitudes are given in the AB system aside from the radio data from ATLAS (Mao et al. 2012; Franzen et al. 2015).
[a]This is in μJy rather than magnitudes.

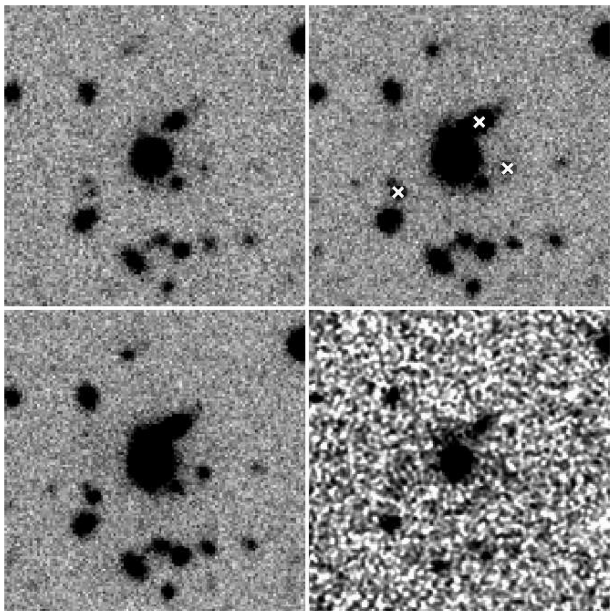

Figure 2. DES images of DES QSO J0330−28 in *g* (topleft), *r* (topright), *i* (bottomleft) and *K* (bottomright). Each box is 30 arcsec on a side centred on the quasar. The *g*, *r* and *i* images are from DES, and the *K*-band image is from the VISTA VIDEO (Jarvis et al. 2013) survey. The three crosses in the *r* image correspond to three sources that have photometric redshifts consistent with DES QSO J0330−28, which suggests a merger.

Telescope Large Array Survey (ATLAS; Franzen et al. 2015; Mao et al. 2012) at 1.474 GHz. If we extrapolate the ATLAS measurement to 5 GHz with a $\alpha = 0.7$, the ratio of rest frame 5 GHz flux density to that at 4400 Å is about 2. This quasar is consequently radio quiet/intermediate under the definition that a ratio less than 1 is quiet and greater than 10 is radio loud. The result is consistent with the idea that LoBALs may be quasars moving between a radio loud and radio quiet phase and some work suggests that the LoBAL fraction in quasars decreases as a function of radio luminosity (Dai, Shankar & Sivakoff 2012). This object unfortunately has no archival

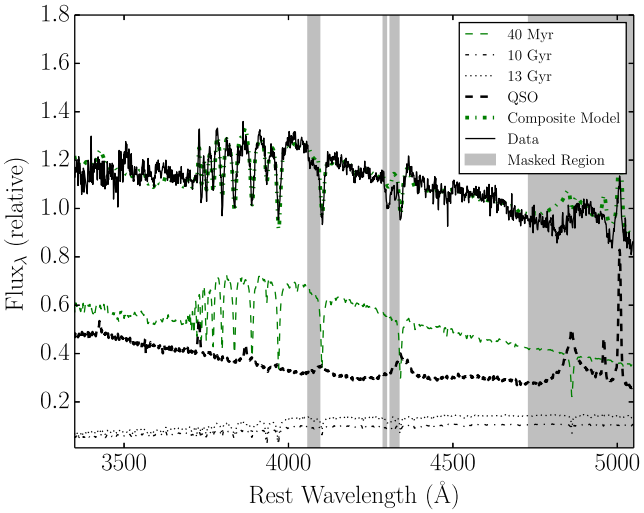

Figure 3. The best-fitting single metallicity model with Z = 0.02 $Z_\odot$. The data (thick solid) are fit by a model (lighter, dot–dashed) that combines a quasar template (dark, dashed) and three major stellar components: 44 per cent of the light comes from a younger, recently quenched population with an age of 40 Myr (lighter, dashed), and 24 per cent comes from older populations of 10 and 13 Gyr (dark dashed and dotted, respectively). The remainder of the light comes from the quasar. The masked regions are left out of the fit due to possible broad quasar emission from H β and broad absorption in the wings of higher order Balmer lines from the quasar. Note that while this low metallicity value is the best fit that we find, this value is not well constrained, as most single-metallicity models find roughly similar light fractions and ages for the young stellar component at a modest increase in $\chi^2_{\rm red}$. At shorter wavelengths, both the post-starburst and quasar components separately overpredict the flux at the base of the BALs. However, no combination of templates and extinction is able to reproduce the flux limits in the absorption lines as well as the normalization of the red half of the spectrum.

Chandra or *XMM–Newton* data, and thus we cannot determine if it is X-ray faint, as has been found for other FeLoBALs (Mathur et al. 1995; Green et al. 2001).

3 ANALYSIS

3.1 Post-starburst

We fit the stacked spectrum with STARLIGHT (Cid Fernandes et al. 2004, 2005a,b) over the wavelength span not dominated by the FeLoBAL's broad absorption and emission lines (see Fig. 3). This corresponds to approximately 3300–4800 Åin the rest frame. We do not fit to longer wavelengths in order to avoid H β contamination, nor shorter wavelengths because of the BALs of the quasar. To account for the quasar component, we created a quasar template from stacked spectra of 10 quasars from the reverberation mapping sample that are most similar in redshift and luminosity to DES QSO J0330−28. We verify that the template created from the OzDES sample is very similar in continuum slope and emission line strength to the SDSS composite quasar from Vanden Berk et al. (2001) and use it in the rest of the analyses.

We initially ran STARLIGHT over a grid of models supplied by Bruzual & Charlot (2003) that span ages of 1 Myr to 13 Gyr and metallicites from 0.005–2.5 $Z_\odot$. The best-fitting model has approximately 45 per cent of the light from two young stellar populations of 40 and 55 Myr, 40 per cent from our quasar template and the remainder from an older population of 6–7 Gyr. The metallicity for the varied components is consistent with subsolar to solar. This fit has $\chi^2_{\rm red}$= 0.85. We also performed fits at single metallicities and found in most instances that between 30 and 50 per cent of the light is from 40 and 55 Myr populations and 20–50 per cent is from the quasar. These fits had $\chi^2_{\rm red}$ranging from 0.9 to 1.2 and show the relative insensitivity of the population ages to the metallicity. The strength of the higher order Balmer lines depths do not match perfectly with any age/metallicity combination. This is likely because of the impact of Balmer absorption in the BAL, and perhaps also some mismatch with the quasar template and this quasar.

For each grid of models, we also fit for the best global extinction and best extinction for each component. The best fits are for A_V = 0–0.04 for nearly all model combinations for both the quasar and post-starburst components. The youngest, single-metallicity solutions are approximately solar, have ages of about 5 Myr, and higher extinction (A_V = 0.37), although these fits are somewhat worse, including to the stellar absorption features. No model is able to reproduce both the spectral shape at 3300–4800 Åand remain below the flux of the absorption troughs. More extinction of both the quasar and post-starburst components would be necessary to not overpredict the flux in the Mg II absorption troughs, but we find no solution that added sufficient reddening to the post-starburst spectrum that did not overpredict the flux redward of 4000 Å. The solution could be underestimated uncertainties in the wavelength-dependent flux calibration of the AAOmega spectra (discussed in Hopkins et al. 2013) and/or that a simple screen is a poor approximation to the dust distribution in the host galaxy. We addressed the first of these two possibilities with additional analyses of spectra obtained at different epochs, which had different and better calibration (Childress, in preparation), but this calibration did not resolve the issues with the fit at short wavelengths.

The mass of the host galaxy from the STARLIGHT fit is $2 \times 10^{11} M_\odot$. Cid Fernandes et al. (2015) found that STARLIGHT stellar mass estimates agree with spectral synthesis estimates to better than 0.4 dex. The uncertainty is likely larger than typical for this QSO, due to the relatively small contribution from the old stellar population, and uncertainties in the extinction.

3.2 BAL QSO

There are a number of absorption troughs present at shorter wavelengths than the stellar absorption features in addition to broad absorption associated with some of the Balmer lines. BAL features are typically described by their balnicity index (BI). This metric originated in Weymann et al. (1991) for HiBALs and the C IV line. By their definition, a quasar was considered a BAL if it had a BI > 0. Later, Hall et al. (2002) proposed the intrinsic absorption index (AI) as an alternative identifier, which is more sensitive to troughs at lower velocities and likewise identifies BALs with AI > 0. Both BI and AI are integrals over velocity on the blue side of an emission line. The BI requires the trough to extend at least 3000 km $s^{-1}$and drop by at least 10 per cent of the normalized continuum flux. The AI, however, begins the integral at 0 km $s^{-1}$and is more sensitive to lower velocity and weaker troughs.

We perform a similar analysis to Hall (2007) for our H β absorption to determine a lower limit column density $N_{\rm H\,\beta} = 5.2 \times 10^{14} {\rm cm}^{-2}$. This value is about a factor of 100 smaller than the column density measurement for the Hall (2007) FeLoBAL, but likely underestimated for DES QSO J0330−28 due to the host galaxy emission at these wavelengths. The H β and Mg II absorption also prohibits a measurement of a black hole mass estimate.

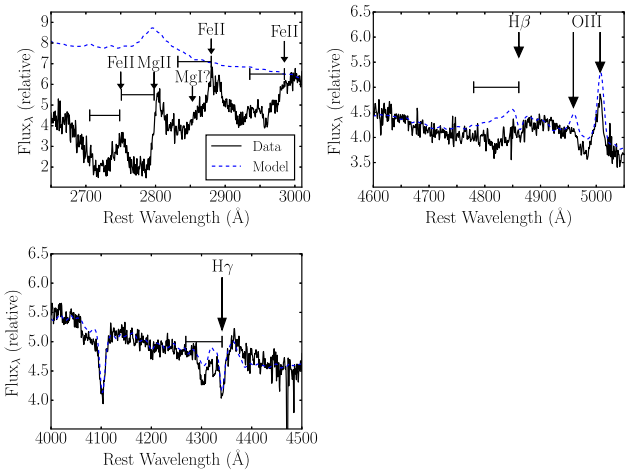

Figure 4. Highlight of the BAL troughs. In each inset, the arrows correspond to the systemic redshift and the horizontal bars correspond to a blueshift velocity of 5000 km s^{-1}. This fits well for Mg II and Fe II, and there is also Balmer absorption that is consistent with this outflow velocity. The dotted line is the best-fitting model for the quasar and stellar components. The model fits well around the Balmer lines, but vastly overestimates the flux at shorter wavelengths.

It is difficult to measure these values in FeLoBALs like DES QSO J0330−28 because these objects have such heavy reddening and the widespread iron absorption/emission makes the continuum poorly defined. The STARLIGHT fit, partially because it could only fit a narrow wavelength range due to the BAL features, has a best-fitting A_V of 0.04. However, DES QSO J0330−28 is clearly highly reddened at shorter wavelengths (see Fig. 1). To correct for this, we applied various values of A_V to our quasar template for an SMC extinction curve (Gordon et al. 2003) until we found the best fit to the red half of the Mg II emission line at 2798 Å. While no single value gives a satisfactory fit to either the extinction or the continuum, the spectral slope on the blue end is broadly consistent with $A_V = 1$–1.5 mag. This is small given how X-ray faint (Green et al. 2001) and red many LoBALs are, but is also poorly constrained by the available data. A likely cause for the difficulty is that there may be partial obscuration; that is, varying amounts of extinction to different regions of the galaxy and quasar emission region. Without a good continuum fit, we cannot reliably measure AI or BI for this object. Nevertheless, the velocity spread of the absorption troughs is reasonably clear. Fig. 4 shows that the Mg II absorption spans approximately 5000 km s^{-1}before a small rise that is likely due to Fe II emission at 2750 Å, which then has its own blueshifted absorption. The depth and width of the trough means that this object would likely meet the conditions for both AI and BI > 0 for Mg II.

We next compare the velocity extent of the Mg II component to other absorption troughs, namely Fe II at 2750, 2880 and 2985 Å, and H β. Fig. 4 shows in both cases the data are consistent with a similar range of blueshifted absorption, and this suggests a common origin.

BALs have a large diversity of spectral morphologies, and DES QSO J0330−28 is most similar to SDSS J112526.13+002901.3 (Hall et al. 2002) with regard to the approximate shape and strength of the emission and absorption features. That SDSS quasar has zero BI, but an intrinsic AI of almost 500 km s^{-1}. While we cannot cleanly measure the continuum of DES QSO J0330−28, it should also have a non-zero intrinsic AI. Hall et al. (2002) also classified SDSS J112526.13+002901.3 as a many narrow troughs FeLoBAL with He I absorption. We do not see evidence for either of these characteristics in DES QSO J0330−28. SDSS J112526.13+002901.3 also does not have the same post-starburst features that make DES QSO J0330−28 unique.

4 DISCUSSION AND CONCLUSION

The current picture for quasar evolution in the merger scenario begins with the collision of a dust- and gas-rich galaxy with another system. Dynamical processes drive material towards the galaxies' centres and fuels star formation and accretion on to the SMBH. The quasar is initially obscured by the dust, but eventually the material disperses and the quasar becomes easily visible. FeLoBALs have attracted particular interest because the very high column density absorption is indicative of a substantial outflow, perhaps associated with this transition from obscured to unobscured. A second scenario proposed by Faucher-Giguère et al. (2012) is that a blast wave is launched from the quasar that impacts a high density cloud along the line of sight. This would also create the observed column densities, reddening and absorption troughs seen in FeLoBALs. One distinction between these scenarios is in where the absorbing material lies. For the transition objects, the absorbing material would be around the quasar and in the process of being blown away, whereas for the blast wave model it is possible to impact a cloud on much larger scales than the central few parsecs.

Variability is one way to test the location of the absorbers. The constraints from several variable FeLoBALs (e.g. Hall et al. 2011; Vivek et al. 2012; McGraw et al. 2015) place the absorbing material of the order of a few to tens of parsecs from the central source. This assumes a cloud-crossing model where the changes arise from an absorber moving across the line of sight. In contrast, other studies suggest the absorption is on kpc scales (Moe et al. 2009; Bautista et al. 2010; Dunn et al. 2010). Moe et al. (2009) derived a distance to one outflow of ∼3 kpc and, for an assumed covering fraction of 0.2, find that the energy in the BAL outflow is comparable to 1 per cent of the total luminosity of the quasar.

We find that the obscuration of DES QSO J0330−28 cannot be fit by a single-screen model. It is clear that the quasar light is highly reddened at the shortest wavelengths, which implies substantial extinction of the AGN accretion disc despite the small A_V of the best fit. We see little to no extinction of the host galaxy in the region over which we fit the models, but extrapolating the stellar population to rest frame 2800 Å and shorter overpredicts the flux in the absorption lines. This implies there is dust in the outer regions of the galaxy as well, though it is not necessarily the same absorption level as the quasar emission, and the discrepancy between the model stellar flux and the absorption trough is greater than for the quasar component. The 'transition object' scenario has this geometry as the young quasar begins to clear out the dust immediately surrounding it to become optically visible. However, such extinction could also arise from a Faucher-Giguère et al. (2012) blast wave colliding with a dense cloud along our line of sight, either close to the AGN or much farther out in the galaxy. For the latter case, the quasar can be highly absorbed and the stellar component less so if there is a low covering fraction of the galaxy-wide absorbers, or both can be reddened if there is a high covering fraction.

If we assume the quasar and starburst triggered simultaneously, we can use the starburst age to evaluate which model FeLoBAL scenario is more probable. Star formation was truncated or quenched in DES QSO J0330−28 around 50 Myr ago in most of our models. This time is comparable to estimates for quasar lifetimes of around 10^{7-8} yr (e.g. Yu & Tremaine 2002; Martini 2004) and implies that this FeLoBAL did not turn on recently, which is in conflict with the young quasar scenario. The FeLoBAL features cannot

be due to the same feedback processes that abruptly ended the star formation ∼50 Myr ago, as they would have dispersed due to Kelvin–Helmholtz or Rayleigh–Taylor instabilities. These features are consistent with the Faucher-Giguère et al. (2012) model in which the absorption is produced by clouds of material that have been compressed by a radiative blast wave. The key aspect of the blast wave model for DES QSO J0330−28 is that the blast wave is not tied to a particular evolutionary phase of the quasar.

We plan to obtain future, higher signal-to-noise ratio spectra over a broader wavelength range to derive better stellar population and reddening parameters. We will also obtain new spectral epochs as the OzDES program progresses, and we will use these data to search for BAL variability to attempt to measure the distance of the absorber from the central source.

ACKNOWLEDGEMENTS

DM would like to gratefully acknowledge the helpful comments by Smita Mathur on a draft of this manuscript.

Funding for the DES Projects has been provided by the U.S. Department of Energy, the U.S. National Science Foundation, the Ministry of Science and Education of Spain, the Science and Technology Facilities Council of the United Kingdom, the Higher Education Funding Council for England, the National Center for Supercomputing Applications at the University of Illinois at Urbana-Champaign, the Kavli Institute of Cosmological Physics at the University of Chicago, the Center for Cosmology and Astro-Particle Physics at the Ohio State University, the Mitchell Institute for Fundamental Physics and Astronomy at Texas A&M University, Financiadora de Estudos e Projetos, Fundação Carlos Chagas Filho de Amparo à Pesquisa do Estado do Rio de Janeiro, Conselho Nacional de Desenvolvimento Científico e Tecnológico and the Ministério da Ciência, Tecnologia e Inovação, the Deutsche Forschungsgemeinschaft and the Collaborating Institutions in the Dark Energy Survey.

The Collaborating Institutions are Argonne National Laboratory, the University of California at Santa Cruz, the University of Cambridge, Centro de Investigaciones Energéticas, Medioambientales y Tecnológicas-Madrid, the University of Chicago, University College London, the DES-Brazil Consortium, the University of Edinburgh, the Eidgenössische Technische Hochschule (ETH) Zürich, Fermi National Accelerator Laboratory, the University of Illinois at Urbana-Champaign, the Institut de Ciències de l'Espai (IEEC/CSIC), the Institut de Física d'Altes Energies, Lawrence Berkeley National Laboratory, the Ludwig-Maximilians Universität München and the associated Excellence Cluster Universe, the University of Michigan, the National Optical Astronomy Observatory, the University of Nottingham, The Ohio State University, the University of Pennsylvania, the University of Portsmouth, SLAC National Accelerator Laboratory, Stanford University, the University of Sussex, Texas A&M University and the OzDES Membership Consortium.

The DES data management system is supported by the National Science Foundation under grant number AST-1138766. The DES participants from Spanish institutions are partially supported by El ministerio de Economia, Industria y Competitividad (MINECO) under grants AYA2012-39559, ESP2013-48274, FPA2013-47986, and Centro de Excelencia Severo Ochoa SEV-2012-0234. Research leading to these results has received funding from the European Research Council under the European Union's Seventh Framework Programme (FP7/2007-2013) including ERC grant agreements 240672, 291329 and 306478.

The data in this paper were based on observations obtained at the Australian Astronomical Observatory.

Part of this research was conducted by the Australian Research Council Centre of Excellence for All-sky Astrophysics (CAASTRO) through project number CE110001020.

REFERENCES

Banerji M. et al., 2015, MNRAS, 446, 2523
Bautista M. A., Dunn J. P., Arav N., Korista K. T., Moe M., Benn C., 2010, ApJ, 713, 25
Becker R. H., Gregg M. D., Hook I. M., McMahon R. G., White R. L., Helfand D. J., 1997, ApJ, 479, L93
Brotherton M. S. et al., 1999, ApJ, 520, L87
Brotherton M. S., Grabelsky M., Canalizo G., van Breugel W., Filippenko A. V., Croom S., Boyle B., Shanks T., 2002, PASP, 114, 593
Bruzual G., Charlot S., 2003, MNRAS, 344, 1000
Cales S. L. et al., 2013, ApJ, 762, 90
Cid Fernandes R., Gu Q., Melnick J., Terlevich E., Terlevich R., Kunth D., Rodrigues Lacerda R., Joguet B., 2004, MNRAS, 355, 273
Cid Fernandes R., González Delgado R. M., Storchi-Bergmann T., Martins L. P., Schmitt H., 2005a, MNRAS, 356, 270
Cid Fernandes R., Mateus A., Sodré L., Stasińska G., Gomes J. M., 2005b, MNRAS, 358, 363
Cid Fernandes R. et al., 2015, in Ziegler B. L., Combes F., Dannerbauer H., Verdugo M., eds, IAU Symp. Vol. 309, Galaxies in 3D across the Universe. Cambridge Univ. Press, Cambridge, p. 93
Coil A. L., Weiner B. J., Holz D. E., Cooper M. C., Yan R., Aird J., 2011, ApJ, 743, 46
Dai X., Shankar F., Sivakoff G. R., 2008, ApJ, 672, 108
Dai X., Shankar F., Sivakoff G. R., 2012, ApJ, 757, 180
Di Matteo T., Springel V., Hernquist L., 2005, Nature, 433, 604
Dressler A., Gunn J. E., 1983, ApJ, 270, 7
Dunn J. P. et al., 2010, ApJ, 709, 611
Dunn J. P. et al., 2015, ApJ, 808, 94
Egami E., Iwamuro F., Maihara T., Oya S., Cowie L. L., 1996, AJ, 112, 73
Farrah D., Lacy M., Priddey R., Borys C., Afonso J., 2007, ApJ, 662, L59
Farrah D. et al., 2010, ApJ, 717, 868
Faucher-Giguère C.-A., Quataert E., Murray N., 2012, MNRAS, 420, 1347
Ferrarese L., Merritt D., 2000, ApJ, 539, L9
Flaugher B., 2005, Int. J. Mod. Phys. A, 20, 3121
Flaugher B. et al., 2015, AJ, 150, 150
Franzen T. M. O. et al., 2015, MNRAS, 453, 4020
Gebhardt K. et al., 2000, ApJ, 539, L13
Gordon K. D., Clayton G. C., Misselt K. A., Landolt A. U., Wolff M. J., 2003, ApJ, 594, 279
Goto T., 2006, MNRAS, 369, 1765
Green P. J., Aldcroft T. L., Mathur S., Wilkes B. J., Elvis M., 2001, ApJ, 558, 109
Hall P. B., 2007, AJ, 133, 1271
Hall P. B., Martini P., DePoy D. L., Gatley I., 1997, ApJ, 484, L17
Hall P. B. et al., 2002, ApJS, 141, 267
Hall P. B., Anosov K., White R. L., Brandt W. N., Gregg M. D., Gibson R. R., Becker R. H., Schneider D. P., 2011, MNRAS, 411, 2653
Hazard C., McMahon R. G., Webb J. K., Morton D. C., 1987, ApJ, 323, 263
Heckman T. M., Best P. N., 2014, ARA&A, 52, 589
Ho I.-T. et al., 2016, MNRAS, 457, 1257
Hopkins A. M. et al., 2013, MNRAS, 430, 2047
Jarvis M. J. et al., 2013, MNRAS, 428, 1281
Kessler R. et al., 2015, AJ, 150, 172
King A. L. et al., 2015, MNRAS, 453, 1701
Komossa S., Burwitz V., Hasinger G., Predehl P., Kaastra J. S., Ikebe Y., 2003, ApJ, 582, L15
Koratkar A., Blaes O., 1999, PASP, 111, 1
Korista K. T., Bautista M. A., Arav N., Moe M., Costantini E., Benn C., 2008, ApJ, 688, 108
Mao M. Y. et al., 2012, MNRAS, 426, 3334

Martini P., 2004, in Ho L. C., ed., Coevolution of Black Holes and Galaxies. Cambridge Univ. Press, Cambridge, p. 169
Mathur S., Elvis M., Singh K. P., 1995, ApJ, 455, L9
McGraw S. M., Shields J. C., Hamann F. W., Capellupo D. M., Gallagher S. C., Brandt W. N., 2015, MNRAS, 453, 1379
McMahon R. G., Banerji M., Gonzalez E., Koposov S. E., Bejar V. J., Lodieu N., Rebolo R., VHS Collaboration, 2013, The Messenger, 154, 35
Moe M., Arav N., Bautista M. A., Korista K. T., 2009, ApJ, 706, 525
Peterson B. M., 1997, An Introduction to Active Galactic Nuclei. Cambridge Univ. Press, Cambridge
Piconcelli E. et al., 2010, ApJ, 722, L147
Sanders D. B., Soifer B. T., Elias J. H., Madore B. F., Matthews K., Neugebauer G., Scoville N. Z., 1988, ApJ, 325, 74
Shakura N. I., Sunyaev R. A., 1973, A&A, 24, 337
Sharp R. G., Bland-Hawthorn J., 2010, ApJ, 711, 818
Sharp R. et al., 2006, in McLean I. S., Iye M., eds, Proc. SPIEConf. Ser. Vol. 6269, Ground-based and Airborne Instrumentation for Astronomy. SPIE, Bellingham, p. 62690G
Silk J., Rees M. J., 1998, A&A, 331, L1
Smith G. A. et al., 2004, in Moorwood A. F. M., Iye M., eds, Proc. SPIEConf. Ser. Vol. 5492, Ground-based Instrumentation for Astronomy. SPIE, Bellingham, p. 410
Tremonti C. A., Moustakas J., Diamond-Stanic A. M., 2007, ApJ, 663, L77
Trump J. R. et al., 2006, ApJS, 165, 1
Urrutia T., Becker R. H., White R. L., Glikman E., Lacy M., Hodge J., Gregg M. D., 2009, ApJ, 698, 1095
Vanden Berk D. E. et al., 2001, AJ, 122, 549
Vivek M., Srianand R., Petitjean P., Noterdaeme P., Mohan V., Mahabal A., Kuriakose V. C., 2012, MNRAS, 423, 2879
Voit G. M., Weymann R. J., Korista K. T., 1993, ApJ, 413, 95
Weymann R. J., Morris S. L., Foltz C. B., Hewett P. C., 1991, ApJ, 373, 23
Wright E. L. et al., 2010, AJ, 140, 1868
Yu Q., Tremaine S., 2002, MNRAS, 335, 965
Yuan F. et al., 2015, MNRAS, 452, 3047
Zabludoff A. I., Zaritsky D., Lin H., Tucker D., Hashimoto Y., Shectman S. A., Oemler A., Kirshner R. P., 1996, ApJ, 466, 104
Zhang S. et al., 2015, ApJ, 815, 113

SUPPORTING INFORMATION

Supplementary data are available at *MNRAS* online.

supplemental_figures_for_referee.tar.gz

Please note: Oxford University Press is not responsible for the content or functionality of any supporting materials supplied by the authors. Any queries (other than missing material) should be directed to the corresponding author for the article.

[1]*Department of Astronomy, The Ohio State University, Columbus, OH 43210, USA*
[2]*Center for Cosmology and Astro-Particle Physics, The Ohio State University, Columbus, OH 43210, USA*
[3]*Australian Astronomical Observatory, 105 Delhi Rd, North Ryde, NSW 2113, Australia*
[4]*Kavli Institute for Cosmology, University of Cambridge, Madingley Road, Cambridge CB3 0HA, UK*
[5]*Institute of Astronomy, University of Cambridge, Madingley Road, Cambridge CB3 0HA, UK*
[6]*School of Mathematics and Physics, University of Queensland, QLD 4072, Australia*
[7]*CAASTRO: ARC Centre of Excellence for All-sky Astrophysics*
[8]*Research School of Astronomy and Astrophysics, Australian National University, Cotter Rd., Weston, ACT 2611, Australia*
[9]*Department of Physics and Astronomy, Curtin University, Kent Street, Bentley, Perth, WA 6102, Australia*
[10]*School of Physics and Astronomy, University of Southampton, Southampton SO17 1BJ, UK*
[11]*Research School of Astronomy and Astrophysics, Australian National University, Canberra, ACT 2611, Australia*
[12]*Sydney Institute for Astronomy, School of Physics, A28, The University of Sydney, NSW 2006, Australia*
[13]*Research School of Astronomy and Astrophysics, Mt. Stromlo Observatory, the Australian National University, Cotter Rd., Canberra, ACT 2611, Australia*
[14]*Cerro Tololo Inter-American Observatory, National Optical Astronomy Observatory, Casilla 603, 1700000 La Serena, Chile*
[15]*Department of Physics and Astronomy, University College London, Gower Street, London WC1E 6BT, UK*
[16]*Department of Physics and Electronics, Rhodes University, PO Box 94, Grahamstown 6140, South Africa*
[17]*Fermi National Accelerator Laboratory, P. O. Box 500, Batavia, IL 60510, USA*
[18]*CNRS, UMR 7095, Institut d'Astrophysique de Paris, F-75014 Paris, France*
[19]*Sorbonne Universités, UPMC Univ Paris 06, UMR 7095, Institut d'Astrophysique de Paris, F-75014 Paris, France*
[20]*Laboratório Interinstitucional de e-Astronomia – LIneA, Rua Gal. José Cristino 77, Rio de Janeiro, RJ 20921-400, Brazil*
[21]*Observatório Nacional, Rua Gal. José Cristino 77, Rio de Janeiro, RJ 20921-400, Brazil*
[22]*Department of Astronomy, University of Illinois, 1002 W. Green Street, Urbana, IL 61801, USA*
[23]*National Center for Supercomputing Applications, 1205 West Clark St, Urbana, IL 61801, USA*
[24]*Institut de Ciències de l'Espai, IEEC-CSIC, Campus UAB, Carrer de Can Magrans, s/n, E-08193 Bellaterra, Barcelona, Spain*
[25]*Institut de Física d'Altes Energies (IFAE), The Barcelona Institute of Science and Technology, Campus UAB, E-08193 Bellaterra, Barcelona, Spain*
[26]*Excellence Cluster Universe, Boltzmannstr. 2, D-85748 Garching, Germany*
[27]*Faculty of Physics, Ludwig-Maximilians-Universität, Scheinerstr. 1, D-81679 Munich, Germany*
[28]*Department of Physics and Astronomy, University of Pennsylvania, Philadelphia, PA 19104, USA*
[29]*Jet Propulsion Laboratory, California Institute of Technology, 4800 Oak Grove Dr., Pasadena, CA 91109, USA*
[30]*Centre for Astrophysics and Supercomputing, Swinburne University of Technology, Hawthorn, VIC 3122, Australia*
[31]*Kavli Institute for Particle Astrophysics and Cosmology, P. O. Box 2450, Stanford University, Stanford, CA 94305, USA*
[32]*SLAC National Accelerator Laboratory, Menlo Park, CA 94025, USA*
[33]*Department of Physics, The Ohio State University, Columbus, OH 43210, USA*
[34]*Institució Catalana de Recerca i Estudis Avançats, E-08010 Barcelona, Spain*
[35]*Centro de Investigaciones Energéticas, Medioambientales y Tecnológicas (CIEMAT), E-28040 Madrid, Spain*
[36]*Instituto de Física, UFRGS, Caixa Postal 15051, Porto Alegre, RS 91501-970, Brazil*
[37]*Department of Physics, University of Michigan, Ann Arbor, MI 48109, USA*
[38]*ICTP South American Institute for Fundamental Research Instituto de Física Teórica, Universidade Estadual Paulista, 01140-070 São Paulo, Brazil*
[39]*Computer Science and Mathematics Division, Oak Ridge National Laboratory, Oak Ridge, TN 37831, USA*
[40]*Institute of Cosmology and Gravitation, University of Portsmouth, Portsmouth PO1 3FX, UK*
[41]*The Research School of Astronomy and Astrophysics, Australian National University, Canberra, ACT 0200, Australia*

This paper has been typeset from a TEX/LATEX file prepared by the author.